

# What Makes a Scene ? Scene Graph-based Evaluation and Feedback for Controllable Generation

Zuyao Chen, Chang Wen Chen  
The Hong Kong Polytechnic University

zuyao.chen@connect.polyu.hk, changwen.chen@polyu.edu.hk

Jinlin Wu, Zhen Lei  
Institute of Automation, CAS  
{wujinlin2017, zhen.lei}@ia.ac.cn

## Abstract

While text-to-image generation has been extensively studied, generating images from scene graphs remains relatively underexplored, primarily due to challenges in accurately modeling spatial relationships and object interactions. To fill this gap, we introduce *Scene-Bench*, a comprehensive benchmark designed to evaluate and enhance the factual consistency in generating natural scenes. *Scene-Bench* comprises *MegaSG*, a large-scale dataset of one million images annotated with scene graphs, facilitating the training and fair comparison of models across diverse and complex scenes. Additionally, we propose *SGScore*, a novel evaluation metric that leverages chain-of-thought reasoning capabilities of multimodal large language models (LLMs) to assess both object presence and relationship accuracy, offering a more effective measure of factual consistency than traditional metrics like FID and CLIPScore. Building upon this evaluation framework, we develop a scene graph feedback pipeline that iteratively refines generated images by identifying and correcting discrepancies between the scene graph and the image. Extensive experiments demonstrate that *Scene-Bench* provides a more comprehensive and effective evaluation framework compared to existing benchmarks, particularly for complex scene generation. Furthermore, our feedback strategy significantly enhances the factual consistency of image generation models, advancing the field of controllable image generation.

## 1. Introduction

“If you can’t measure it, you can’t improve it.”

– Peter Drucker

Generating realistic images coherent with natural scenes is important in numerous applications such as photo edit-

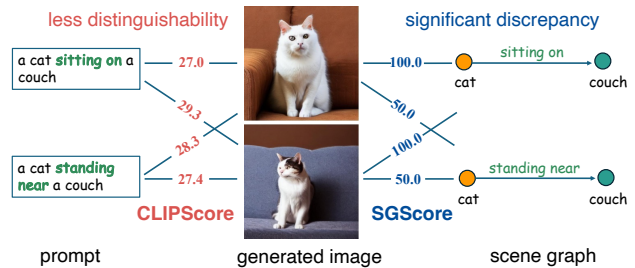


Figure 1. A comparison of CLIPScore [18] and the proposed SGScore for evaluating factual consistency. SGScore can distinguish such relationship discrepancies, while CLIPScore often overlooks them.

ing [21, 25, 61], content creation [4, 24, 44], etc. Early generative models like Variational Autoencoders (VAE) [26] produced blurry images due to limitations in modeling complex data distributions. Generative Adversarial Networks (GAN) [16] improved image quality but faced issues like training instability and mode collapse. Recently, diffusion models like Stable Diffusion [44] have proven effective for generating visually appealing images with realistic objects and high-resolution details [11, 20, 38, 40]. Although diffusion models have achieved significant success, they still face challenges in generating complex scenes involving multiple objects [34, 55], particularly in ensuring factual consistency, such as the accurate presence of multiple objects and the correct relationship between objects within a natural image.

Recent efforts have aimed to address these limitations, focusing on compositional objects [14, 35, 36], improving text-image alignment [12, 29], and enhancing spatial consistency [6]. For instance, methods like Composable Diffusion [35] compose multiple concepts by explicitly optimizing the defined energy functions, and Structured Diffu-

sion [14] combines multiple objects by manipulating cross-attention layers. These methods improve the accuracy of multiple objects occurring in a single scene. Additionally, Chatterjee [6] proposed a benchmark to evaluate and enhance the capability of modeling spatial relationships.

Despite this progress, **how to evaluate the factual consistency between the condition (e.g., text, image, etc.) and the generated image** remains challenging. The difficulty lies in standard metrics like Fréchet Inception Distance (FID) [19] and CLIPScore [18] primarily evaluate image quality but fall short in capturing factual consistency in complex scenes. FID, widely used to assess the visual fidelity of generated images, focuses on feature distribution matching between real and generated datasets. However, it overlooks spatial relationships and object interactions. For instance, images depicting a dog “under a table” and “on a table” may receive similar FID scores, despite their vastly different relationships. Similarly, CLIPScore measures semantic alignment between images and text by emphasizing global themes but cannot assess specific object relationships. CLIPScore may assign high scores to images that include all relevant objects but incorrectly depict their relationships, such as confusing “a cat sitting on a couch” with “a cat standing near a couch” (see Fig. 1). The drawback of FID and CLIPScore highlights the need for more specialized evaluation metrics to assess objects’ presence and precise interactions between them.

To evaluate the factual consistency, we employ a structured representation known as a *Scene Graph*, which has been demonstrated to outperform pure text in image retrieval [22, 27]. A scene graph encodes objects as nodes and their relationships as edges. For textual conditions, scene graphs can be parsed using natural language processing tools such as Scene Parser [37] or large language models (LLMs). For image conditions, scene graphs are generated via Scene Graph Generation (SGG) models [10, 48, 52, 58] or multimodal LLMs. Leveraging this structured representation, we introduce a novel evaluation metric, **SGScore**, which quantifies the factual consistency between generated images and their corresponding scene graphs. SGScore evaluates *Object Recall* by verifying the presence of nodes and *Relation Recall* by assessing the accuracy of edges within the scene graph. To adapt different domains and handle the extensive vocabulary inherent in generated images, we utilize a multimodal LLM to perform these evaluations instead of relying on a pre-trained SGG model to convert images into scene graphs. Thanks to the chain-of-thought reasoning and zero-shot capabilities of the multimodal LLM, SGScore can effectively distinguish between images depicting subtle differences, as shown in Fig. 1.

When applying the new metric to benchmark different generative models, a critical bottleneck is the lack of large-scale datasets annotated with scene graphs, which are es-

sential for fair and comprehensive comparisons. Existing datasets, such as Visual Genome (VG) [27] and COCO-Stuff [5], are relatively small (e.g., only 5k and 2k images for testing, respectively), and their inherent long-tail distributions lead to unfair and biased evaluations. As a result, we develop **MegaSG**, a large-scale dataset comprising one million images richly annotated with scene graphs that capture a wide range of objects and their complex relationships. MegaSG enables models to be trained and evaluated on diverse scenarios, from simple to highly intricate scenes, thus overcoming the limitations of previous datasets that were constrained by small-scale and biased distributions.

By combining the proposed *SGScore* and *MegaSG*, we introduce a novel benchmark, **Scene-Bench**. To provide a comprehensive and fair benchmark, we sample images from MegaSG based on Scene Diversity and Scene Complexity. Scene Diversity sampling aims to evaluate model performance across diverse scene scenarios, while Scene Complexity sampling aims to evaluate model performance at different complexity levels. To our knowledge, *Scene-Bench* is the first benchmark to evaluate generative models on a large-scale natural scene dataset using scene graphs.

Building upon this scene graph-based evaluation, we design a scene graph feedback pipeline that leverages multimodal LLMs for iterative refinement. The process begins with generating an initial image from a scene graph, followed by assessing factual consistency using the *Scene-Bench* metrics. When discrepancies are detected, such as missing objects or incorrect relationships, a missing graph is created to highlight these errors. A reference image is generated based on this missing graph to address the identified issues. By integrating this new image with the initial one, we refine the output, resulting in a final image that more accurately matches the intended scene described by the original scene graph.

In short, our contribution can be summarized as

- We introduce *Scene-Bench*, a comprehensive and large-scale benchmark for evaluating factual consistency using scene graphs. *Scene-Bench* includes *MegaSG*, a dataset with one million images annotated with scene graphs, and a novel evaluation metric, *SGScore*, which explicitly measures factual consistency by assessing the accuracy of object presence and relationships in generated images.
- We propose a scene graph feedback strategy that iteratively refines generated images by detecting and correcting discrepancies in object presence and relationship accuracy, thereby enhancing the factual consistency between the generated image and the intended scene.
- Extensive experiments demonstrate that *Scene-Bench* provides a more comprehensive and effective evaluation benchmark for factual consistency in natural scenes. Furthermore, our proposed feedback pipeline significantly improves the factual consistency of generated images,

particularly in complex scene scenarios.

## 2. Related Work

**Text-to-Image Generation.** The field of text-to-image generation has seen significant advancements with the transition from GANs [17] to diffusion models. Early GAN-based methods like StackGAN [59] and AttnGAN [53] generated images from textual descriptions but often struggled with image quality and diversity. The introduction of diffusion models marked a substantial improvement. Models such as DALL-E [42], GLIDE [38], and Stable Diffusion [44] have achieved high-quality image synthesis with better text-image alignment by iteratively refining images from noise, conditioned on text prompts. Despite their success, these models face challenges in generating complex scenes involving multiple objects and ensuring consistency in object relationships.

**Scene Graph-to-Image Generation.** Scene graphs offer a structured representation of objects and their relationships, providing a promising scheme for controllable image generation. Johnson *et al.* [23] introduced SG2Im, a model that generates images from scene graphs using graph convolutional networks (GCN) and conditional GANs. Ashual and Wolf [3] extended this approach by incorporating more detailed scene representations and object attributes. Recent methods have integrated scene graphs with diffusion models to enhance compositionality [33, 35]. However, these approaches often require large-scale scene graph datasets and rely on additional guidance like bounding boxes [13] or specialized graph encoders, which cannot be adapted to open vocabulary. The evaluation of these models remains a challenge due to the lack of metrics that capture the fidelity of object relationships in generated images.

**Large Language Models in Image Generation.** The integration of LLMs has opened new possibilities in image generation. Recent works have leveraged LLMs to enhance compositionality and controllability in image synthesis. For example, LayoutGPT [15] utilizes LLMs as visual planners to generate layouts from textual descriptions, improving user controllability. Similarly, methods like RPG [55] and Complex Diffusion [34] leverage the chain-of-thought reasoning capabilities of LLMs to decompose complex prompts into simpler tasks, aiding in the generation of complex scenes with multiple objects and relationships. However, their potential for providing feedback to iteratively refine scene graph-based generation has not been fully explored.

**Improving Relationship Consistency.** Addressing the limitations in capturing object relationships, several approaches have been proposed. Feng *et al.* [14] focused on improving compositional generalization in diffusion models through a modulated cross-attention mechanism. Park *et al.* [39] introduced benchmarks specifically targeting com-

positional understanding in generative models. Chatterjee *et al.* [6] designed a benchmark to evaluate the capability of modeling spatial relationships. Despite these efforts, ensuring accurate depiction of relationships in complex scenes remains a significant challenge, and existing methods often do not provide mechanisms for iterative refinement based on explicit relationship feedback.

## 3. Scene-Bench

Scene-Bench is designed for evaluating and enhancing the factual consistency in generating natural scenes, in terms of objects and relationships. Specifically, Scene-Bench consists of a large-scale dataset of scene graphs, and an autonomous evaluation pipeline.

### 3.1. MegaSG: a large-scale dataset of scene graphs

**Creation of the Dataset.** Due to the complexity and high cost of manual annotation, existing scene graph datasets, such as Visual Genome [27], are relatively small in scale (*e.g.*, only 5k images are prepared for the test set [23]). The limited size and inherent long-tail distribution make these datasets inadequate for studying diffusion models across diverse scene scenarios. To address this limitation and build a large-scale scene graph dataset, we leverage the chain-of-thought reasoning capabilities of multimodal large language models (LLMs) in combination with pre-existing object detection datasets. Specifically, we collect **1 million** images from COCO [8], Object365 [46], and Open Images v6 [28], which offer rich object categories and bounding boxes. These datasets are ideal for generating large-scale scene graphs efficiently.

As shown in Fig. 2, the multimodal LLM takes an image with object categories and bounding boxes as input and generates a scene graph that describes the relationships between objects. For instance, in the provided example, the model identifies a “person” kicking a “sports ball” and another “person” nearby, resulting in the following scene graph: {“source”: “person.2”, “target”: “sports ball.1”, “relation”: “kicking”}, {“source”: “person.2”, “target”: “person.3”, “relation”: “near”}. This structured representation captures both the objects and their spatial and relational interactions.

**Scene Diversity.** To better understand the behavior of diffusion models in diverse scene scenarios, we utilized an LLM (*e.g.*, Gemini 1.5 Flash [43]) to classify the MegaSG dataset into two main themes: *People-Centric* and *Non-People-Centric*. The *People-Centric* theme includes fine-grained categories such as *Social Interaction*, *Individual Activities*, *Work / Occupation*, *Travel / Exploration*, *Sports & Recreation*, *Performance / Entertainment*, *Daily Life*. For the *Non-people-Centric* theme, we identified categories like *Nature*, *Urban / Built*, *Objects*, and *Abstract / Artistic*. The hierarchical distribution of these categories is illustrated in

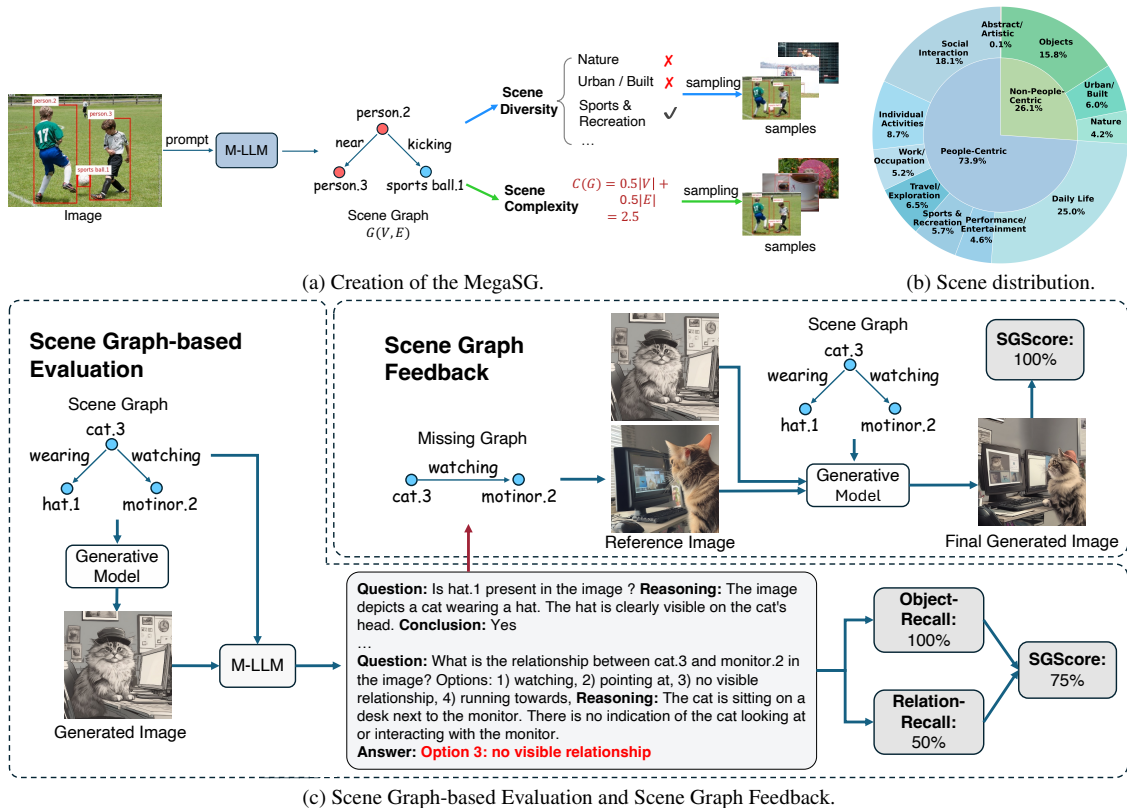


Figure 2. Overview of the Scene-Bench. (a) Scene graphs are generated from images using a multimodal LLM (M-LLM), capturing object relationships and interactions. Scene Diversity and Scene Complexity guide sampling to ensure dataset balance. (b) Scene distribution across categories highlights the diversity in People-Centric and Non-People-Centric themes. (c) Scene graph-based evaluation and feedback leverages the M-LLM to calculate object and relationship recall, generating an SGScore metric that quantifies factual consistency between the generated image and the intended scene. The feedback identifies and corrects discrepancies, iteratively refining the generated image.

Dataset	Images	Vocabulary Diversity	Test		
			Samples	Triples	Complexity Balanced
VG [27]	108k	179 objects, 49 relations	5,096	12.8k	✗
COCO-Stuff [5]	4.5k	171 objects, 6 relations	2,048	22.7k	✗
MegaSG	1M	775 objects, 122 relations	50,000	275k	✓

Table 1. Comparison of MegaSG with existing scene graph datasets.

Fig. 2 (b). And samples are shown in the figure (see **Supplementary materials**), showcasing the diversity and range of scenarios covered in the dataset.

**Scene Complexity.** In addition to categorizing natural scenes, measuring scene complexity is crucial for evaluating the performance of diffusion models. While simple scenes are generally easier for these models to handle, complex scenes pose greater challenges. This raises an important question: *How can we quantitatively define the complexity of a natural scene?*

In this work, we define the complexity of a scene based on its scene graph  $G = (V, E)$ , where  $V$  represents the set

of nodes (objects) and  $E$  represents the set of edges (relationships). The complexity is calculated as

$$C(G) = \gamma \cdot |V| + (1.0 - \gamma) \cdot |E|, \quad (1)$$

where  $\gamma \in [0, 1]$  is a weighting factor that balances the influence of the number of nodes and edges.

The scene graph representation provides a straightforward way to quantify complexity, making it possible to analyze the performance of diffusion models across a range of difficulty levels, from simple to highly complex scenes. In contrast, defining the complexity of a text prompt is inherently more challenging due to the lack of explicit struc-

tural information. By leveraging this graph-based approach, we can better understand how diffusion models respond to varying levels of scene complexity, offering insights into their strengths and limitations across different scenarios.

**Dataset Comparison.** We compare the MegaSG with existing scene graph datasets, specifically Visual Genome (VG) [27] and COCO-Stuff [5], as summarized in Tab. 1. MegaSG significantly outperforms VG and COCO-Stuff in terms of scale, encompassing 1 million images compared to VG’s 108k and COCO-Stuff’s 4.5k. Additionally, MegaSG offers a substantially richer vocabulary with 775 object categories and 122 relations, enhancing the diversity and complexity of scene annotations. Importantly, MegaSG’s test set is *complexity balanced*, ensuring an even distribution of simple, medium, and hard scenes, whereas VG and COCO-Stuff lack this balanced composition.

To quantitatively verify the quality of MegaSG, we evaluate Scene Graph Generation (SGG) models trained on different datasets. For instance, the OvSGTR (Swin-B) [10] model trained on MegaSG achieves a zero-shot performance recall of 45.71% (R@50, PredCls mode) on the VG150 test set, outperforming models trained on smaller datasets like COCO Caption data (see **Supplementary Materials**). This improvement reflects the high-quality scene graph annotations of MegaSG, enabling further exploration of training SGG models on MegaSG or generating images from scene graphs on MegaSG.

### 3.2. Evaluation Strategy

To quantify the factual consistency, we utilize a multimodal LLM (M-LLM) to assess the recall of objects and relationships, as shown in Fig. 2 (c).

**Recall of Objects.** Given a generated image  $I$  and its intended scene graph  $G = (V, E)$ , where  $V$  represents the set of objects (nodes) and  $E$  represents the relationships (edges), we prompt the M-LLM with specific queries about the existence of each object. For example, for a scene graph containing the relationships:  $\{“source”: “person.2”, “target”: “sports ball.1”, “relation”: “kicking”\}$ ,  $\{“source”: “person.2”, “target”: “person.3”, “relation”: “near”\}$ , we would prompt the M-LLM with questions such as “*Is there a sports ball in the image?*”. The M-LLM, based on its multimodal capabilities, examines the generated image and responds with a binary answer (Yes / No) to indicate whether the specified object is present. We define the object recall as the fraction of correctly identified objects in the generated image:

$$\text{ObjectRecall}(G, I) = \frac{|V_{\text{pred}} \cap V_{\text{gt}}|}{|V_{\text{gt}}|}, \quad (2)$$

where  $V_{\text{pred}}$  is the set of objects the LLM identifies as present in the image, and  $V_{\text{gt}}$  is the set of ground-truth objects from the original scene graph.

**Recall of Relationships.** To further assess the quality of the generated scene, we evaluate the recall of relationships between objects in the image. For each relationship  $r \in E$ , we check whether the predicted relationship  $r_{\text{pred}}$  exists between the corresponding objects in the generated image. The relationship recall is defined as:

$$\text{RelationRecall}(G, I) = \frac{|E_{\text{pred}} \cap E_{\text{gt}}|}{|E_{\text{gt}}|}, \quad (3)$$

where  $E_{\text{pred}}$  represents the predicted relationships between objects in the generated scene, and  $E_{\text{gt}}$  represents the ground-truth relationships from the original scene graph. To obtain  $E_{\text{pred}}$ , we prompt the LLM with multiple-choice questions such as: “*What is the relationship between the person and the sports ball in the image? A) kicking; B) throwing; C) holding; D) no visible relationship.*”

**SGScore.** In addition to individual recalls of objects and relationships, we introduce a comprehensive metric, *SGScore*, which evaluates the overall quality of the scene graph in terms of both objects and relationships. *SGScore* is computed as a weighted combination of object recall and relationship recall:

$$\text{SGScore}(G, I) = \alpha \cdot \text{ObjectRecall}(G, I) + (1.0 - \alpha) \cdot \text{RelationRecall}(G, I), \quad (4)$$

where  $\alpha \in [0, 1]$  is a hyperparameter that controls the relative importance of object recall versus relationship recall. By adjusting this weight, we can tune the evaluation to place more emphasis on either the objects or the relationships, depending on the task requirements. *SGScore* provides a holistic evaluation of how well the generated scene aligns with the scene graph, offering a balanced measure that reflects both object accuracy and relationship consistency.

## 4. Scene Graph Feedback

Building on the scene graph-based evaluation, we propose a scene graph feedback to iteratively refine the generated image based on identified discrepancies between the image and the input scene graph. This process leverages multimodal LLMs to analyze the generated scene and provide targeted feedback for refinement.

Specifically, given a scene graph  $G = (V, E)$ , we first perform scene composition using an LLM, in which nodes and edges are seamlessly integrated into a *prompt* for an exact scene. This *prompt* results in an initial image  $I_0$  through the diffusion model  $f_D$ . With the input scene graph  $G$  and the generated image  $I_0$ , a multimodal LLM  $f_M$  has been applied to evaluate the presence of objects and relationships. The missing objects and relationships are constructed as a missing graph  $G_{\text{miss}}$ . If discrepancies exist, e.g.,  $G_{\text{miss}} \neq (\emptyset, \emptyset)$ , we will generate a reference image

$I_1$  conditioned on the  $G_{\text{miss}}$  as does in generating  $I_0$  conditioned on  $G$ . To generate the final output image, we use IP-Adapter [56] to integrate  $\text{prompt}$ ,  $I_0$ , and  $I_1$ , in which the cross attention process can be formulated as

$$\begin{aligned} Z = & \text{Attention}(Q, K_{\text{prompt}}, V_{\text{prompt}}) + \\ & \lambda_0 \cdot \text{Attention}(Q, K_{I_0}, V_{I_0}) + \\ & \lambda_1 \cdot \text{Attention}(Q, K_{I_1}, V_{I_1}), \end{aligned} \quad (5)$$

where  $Q$  is the query features of the latent variable,  $K_{\text{prompt}} / V_{\text{prompt}}$ ,  $K_{I_0} / V_{I_0}$ ,  $K_{I_1} / V_{I_1}$ , are the projected features of  $\text{prompt}$ ,  $I_0$ ,  $I_1$ , respectively. The Attention is defined as  $\text{Attention}(Q, K, V) = \text{softmax}(\frac{QK^T}{\sqrt{d}})V$  as does in [49].  $\lambda_0, \lambda_1$  are weight factors.

## 5. Experiments

### 5.1. Experimental Setup

**Models.** We evaluate several popular diffusion models on Scene-Bench, including variants of Stable Diffusion and other state-of-the-art methods.

**Datasets.** We use the Visual Genome dataset [27] following the data splits from SG2Im [23], and the proposed MegaSG dataset. For a fair comparison, we balance samples for testing based on Scene Diversity and Scene Complexity (see *supplementary materials*).

**Metrics.** We employ common metrics such as Inception Score (IS) [45], Fréchet Inception Distance (FID) [19], and CLIPScore [18]. Additionally, we introduce ObjectRecall, RelationRecall, and SGScore (see Sec. 3.2 and *supplementary materials* for details).

**Scene Graph Representation and Complexity.** For text-to-image models, we format the scene graphs as “{subject} {predicate} {object}” (e.g., *cat sitting on desk, dog near chair*). Based on Scene complexity defined as Eq. (6), we categorize the scene complexity into three levels: **simple**, **medium**, and **hard** (details in *supplementary materials*).

**LLM.** We use Gemini 1.5 Flash [43] (cutoff November 2024) as the multimodal LLM in our experiments. We also report results using local multimodal LLMs like LLaVA [32] in *supplementary materials*.

### 5.2. Evaluation of Scene-Bench

**Performance on Visual Genome.** Table 2 presents the results on the VG test set. The first finding is that *SGScore* provides much more distinguishability than other metrics like FID and CLIPScore. For instance, SD v1.5 has a better FID score than SD v2.1 (42.8 vs. 46.6), yet its *SGScore* is lower than that of SD v2.1 (52.5 vs. 54.4), indicating there are more missed objects and relationships in the images generated by SD v1.5. Another finding is that due to the VG test set being biased towards simple scenes, the performance on medium and hard scenes is counterintuitive:

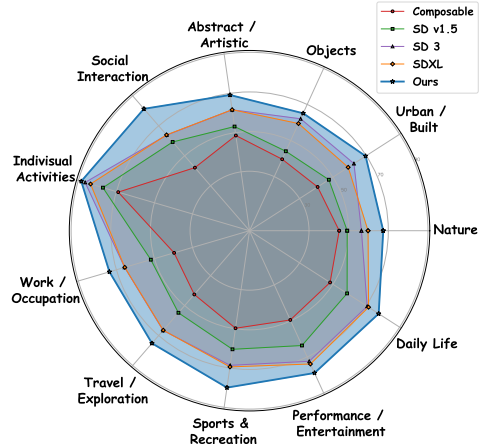


Figure 3. Comparison of model performances using SGScore across various scene categories.

the performance should decrease as scene complexity increases, but this trend is not consistently observed, largely because of the limited number of complex scenes in the test set. This counterexample justifies why we need a new large-scale benchmark to evaluate models comprehensively.

**Performance on MegaSG.** To fairly assess models’ abilities to handle more complex scenes, we evaluated them on a large-scale subset of the MegaSG dataset, sampled by Scene Complexity ( $\gamma = 0$ ). As shown in Tab. 3, we observe a general decline in performance across all models. For example, SD v1.5’s *SGScore* drops from 64.9 (simple scenes) to 44.7 (hard scenes), indicating they struggle more with accurately modeling the relationships in complex scenes.

**Performance Across Scene Diversity.** We evaluated model performance across diverse scene categories identified in our Scene Diversity analysis (see Section 3.1). Fig. 3 presents results for categories like *Social Interaction*, *Nature*, and *Urban Environments*. Models generally perform better in categories like *Individual Activities*, *Performance / Entertainment*, and *Daily Life*, but face challenges in *Social Interaction* (where scenes often include multiple people) and *Abstract / Artistic* (due to style discrepancies), etc. This variation underscores the importance of evaluating models across a broad range of scenarios to comprehensively assess their strengths and limitations.

**Impact of Scene Complexity.** Beyond the three coarse levels of scene complexity, we analyze the effect of scene complexity ranging from 1 to 10 on model performance. For more details, please see *Supplementary materials*.

### 5.3. Evaluation of Scene Graph Feedback

We evaluated our scene graph feedback pipeline using two diffusion models: SD v1.5 [44] and SDXL [40]. For each model, we compared three settings: baseline (without scene composition or feedback), with scene composition only, and

Method	Resolution	IS $\uparrow$	FID $\downarrow$	CLIPScore $\uparrow$	SGScore $\uparrow$			
					Overall	Simple (# 3993)	Medium (# 930)	Hard (# 173)
SGDiff [54]	256x256	16.0	29.6	-	64.5	64.2	66.3	61.5
SceneGenie [13]	256x256	20.2	42.2	-	-	-	-	-
Composable [35]	512x512	20.5	47.5	22.0	48.0	48.9	45.0	44.5
Structured [14]	512x512	23.0	42.2	22.0	52.5	51.8	54.6	56.1
SD v1.5 [44]	512x512	23.1	42.8	22.0	52.5	51.9	54.7	53.9
SD v2.1 [44]	768x768	20.8	46.6	22.1	54.4	53.5	57.8	57.9
PixArt- $\alpha$ [7]	1024x1024	20.8	52.9	22.1	59.8	58.5	64.1	67.0
SD3.5 [11]	1024x1024	21.5	45.6	22.1	60.5	59.4	64.1	65.9
SD3 [11]	1024x1024	23.4	44.5	22.1	62.1	60.9	66.3	66.7
SDXL [40]	1024x1024	23.1	43.4	22.1	60.7	59.6	64.0	69.6
RPG [55] (SDXL)	1024x1024	22.9	44.2	19.3	69.3 (+14.2%)	69.4 (+16.4%)	68.7 (+7.3%)	70.5 (+1.3%)
Ours (SD v1.5)	512x512	20.7	41.6	19.1	65.1 (+24.0%)	65.1 (+25.4%)	65.1 (+19.0%)	66.8 (+23.9%)
Ours (SDXL)	1024x1024	21.0	42.7	19.3	74.1 (+22.1%)	74.2 (+24.5%)	73.3 (+14.5%)	75.3 (+8.2%)

Table 2. Model Comparison on the VG test set. Models including SGDiff and SceneGenie are trained on VG train set. Since SceneGenie [13] does not release the code, we only present the reported IS and FID.

Method	Resolution	IS $\uparrow$	FID $\downarrow$	CLIPScore $\uparrow$	SGScore $\uparrow$			
					Overall	Simple (# 15k)	Medium (# 20k)	Hard (# 15k)
Composable [35]	512x512	20.3	41.0	22.9	42.0	61.0	39.0	28.3
Structured [14]	512x512	28.6	26.2	23.0	53.9	65.1	53.9	46.0
SD v1.5 [44]	512x512	27.0	29.1	22.8	54.2	64.9	53.4	44.7
SD v2.1 [44]	768x768	24.9	34.0	22.9	57.8	68.2	56.4	49.2
PixArt- $\alpha$ [7]	1024x1024	24.3	43.9	23.0	59.5	68.4	58.2	52.7
SD3.5 [11]	1024x1024	25.9	34.5	23.0	63.4	73.1	61.9	55.7
SD3 [11]	1024x1024	27.2	35.5	23.0	65.2	74.2	63.8	58.0
SDXL [40]	1024x1024	25.3	31.6	23.0	65.6	72.9	64.6	59.6
RPG [55] (SDXL)	1024x1024	23.4	37.5	20.0	71.0 (+8.2%)	76.5 (+4.9%)	70.5 (+9.1%)	66.1 (+10.9%)
Ours (SD v1.5)	512x512	23.1	28.9	19.9	62.0 (+14.4%)	71.0 (+9.4%)	61.3 (+14.8%)	53.9 (+20.6%)
Ours (SDXL)	1024x1024	21.6	34.1	20.0	77.1 (+17.5%)	81.8 (+12.2%)	76.6 (+18.6%)	73.1 (+22.7%)

Table 3. Model comparison on a 50,000-image subset of the MegaSG dataset, sampled with a Scene Complexity of  $\gamma = 0$ . Scene graph-based methods such as SGDiff [54], which are limited by the vocabulary of the VG dataset, were excluded from testing.

with both scene composition and feedback.

**Results and Analysis.** Table 4 summarizes the results. For SD v1.5, the baseline achieved an ObjectRecall of 64.93% and a RelationRecall of 44.19% (SGScore 54.56%). Incorporating scene composition improved these metrics to 75.45% and 48.84% (SGScore 62.14%), demonstrating that detailed prompts help the model better capture specified objects and relationships. Applying our feedback strategy further increased ObjectRecall to 79.93% and RelationRecall to 53.97% (SGScore 66.95%), indicating effective correction of discrepancies. A similar trend was observed in SDXL, where improvements after applying scene composition and feedback increased the SGScore from 65.50% to 77.25%.

Compared with LLM-based methods like RPG [55], the performance gain on VG or MegaSG is significant. RPG [55] utilizes an LLM as an agent to perform recaptioning, region planning and merging, while it lacks a feedback for ensuring factual consistency.

These results demonstrate that our scene graph feedback effectively enhances factual consistency by identifying and correcting discrepancies between generated images and the

Model	ObjectRecall $\uparrow$	RelationRecall $\uparrow$	SGScore $\uparrow$
SD v1.5 [44]			
Baseline	64.93 $\pm$ 0.31	44.19 $\pm$ 0.09	54.56 $\pm$ 0.12
+ Scene Composition	75.45 $\pm$ 0.19	48.84 $\pm$ 0.39	62.14 $\pm$ 0.25
+ Feedback	<b>79.93 <math>\pm</math> 0.34</b>	<b>53.97 <math>\pm</math> 0.20</b>	<b>66.95 <math>\pm</math> 0.23</b>
SDXL [40]			
Baseline	77.22 $\pm$ 0.22	53.78 $\pm$ 0.36	65.50 $\pm$ 0.19
+ Scene Composition	88.07 $\pm$ 0.17	60.37 $\pm$ 0.14	74.22 $\pm$ 0.14
+ Feedback	<b>91.30 <math>\pm</math> 0.24</b>	<b>63.20 <math>\pm</math> 0.10</b>	<b>77.25 <math>\pm</math> 0.21</b>

Table 4. Effectiveness of the scene graph feedback on 5,000 images sampled from MegaSG.

intended scene graphs.

## 5.4. Qualitative Evaluation

We present qualitative results to demonstrate the effectiveness of Scene-Bench and the proposed scene graph feedback. Fig. 4 compares images generated by various models using the same scene graphs. Most of models often struggle with complex scenes, leading to images with missing objects or incorrectly depicted relationships. For example, when generating a scene from the scene graph



Figure 4. Comparison of Scene Graph-based Image Generation across Different Models. Each row displays a unique scene graph used as input for image generation. We present the **SGScore** below each generated image to quantify the consistency between the scene graph and the generated output.

$\langle \text{person.2, holding, baseball glove.1} \rangle$ ,  $\langle \text{person.3, wearing, helmet.4} \rangle$ , previous models may omit the *helmet* or fail to represent *person wearing helmet*.

With the proposed scene graph feedback, the generated image more faithfully represents the intended scene graph. The feedback process identifies missing elements and corrects relational inaccuracies, resulting in the image where one person is wearing a helmet and another is holding a baseball glove. This demonstrates the model’s improved ability to handle complex object interactions and spatial arrangements, highlighting the benefits of our approach.

### 5.5. Human Evaluation

We perform a human evaluation to demonstrate how **SGScore** enhances factual consistency verification. To this end, annotators are tasked with answering 1,000 four-to-one questions (examples can be found in *Supplementary materials*). Each question presents an original image alongside four generated images from different models, and annotators are asked to choose the image that best aligns with the original in terms of object presence and relationships. The results, as shown in Fig. 5, demonstrate a clear preference for our model over others, both by human annotators and machine selections. This preference indicates a higher factual consistency of images generated by our model, as de-

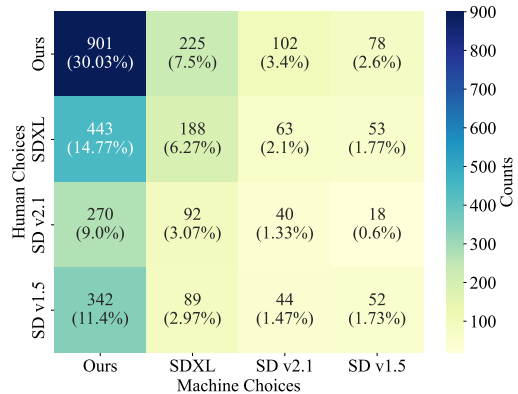


Figure 5. Confusion matrix showing the comparison of human choices against machine choices based on **SGScore**.

termined by **SGScore**.

### 6. Conclusion

In this work, we introduced *Scene-Bench*, a comprehensive and large-scale benchmark designed to evaluate factual consistency in the generation of natural scenes. *Scene-Bench* includes the large-scale *MegaSG* dataset and a novel evaluation metric, **SGScore**, which assesses object pres-



ence and relationship accuracy using multimodal large language models. The proposed scene graph feedback leverages explicit evaluations to iteratively refine generated images, significantly improving factual consistency. Extensive experiments demonstrate that *Scene-Bench* provides a rigorous evaluation framework, particularly excelling in complex scene scenarios where traditional metrics fall short. By effectively addressing the challenges of accurately modeling spatial relationships and object interactions, the proposed scheme advances the field of controllable generation and sets a new benchmark for future research.

## References

- [1] Josh Achiam, Steven Adler, Sandhini Agarwal, Lama Ahmad, Ilge Akkaya, Florencia Leoni Aleman, Diogo Almeida, Janko Altenschmidt, Sam Altman, Shyamal Anadkat, et al. Gpt-4 technical report. *arXiv preprint arXiv:2303.08774*, 2023. 14, 16
- [2] Google AI. Gemini 1.5 flash pricing. [https://ai.google.dev/pricing#1\\_5flash](https://ai.google.dev/pricing#1_5flash), 2024. 16
- [3] Oron Ashual and Lior Wolf. Specifying object attributes and relations in interactive scene generation. In *ICCV*, pages 4561–4569, 2019. 3
- [4] Andrew Brock, Jeff Donahue, and Karen Simonyan. Large scale GAN training for high fidelity natural image synthesis. In *ICLR*, 2019. 1
- [5] Holger Caesar, Jasper Uijlings, and Vittorio Ferrari. Cocomp: Thing and stuff classes in context. In *CVPR*, pages 1209–1218, 2018. 2, 4, 5
- [6] Agneet Chatterjee, Gabriela Ben Melech Stan, Estelle Aflalo, Sayak Paul, Dhruva Ghosh, Tejas Gokhale, Ludwig Schmidt, Hannaneh Hajishirzi, Vasudev Lal, Chitta Baral, and Yezhou Yang. Getting it right: Improving spatial consistency in text-to-image models. In *ECCV*, pages 204–222, 2024. 1, 2, 3
- [7] Junsong Chen, Jincheng Yu, Chongjian Ge, Lewei Yao, Enze Xie, Zhongdao Wang, James T. Kwok, Ping Luo, Huchuan Lu, and Zhenguo Li. PixArt- $\alpha$ : Fast training of diffusion transformer for photorealistic text-to-image synthesis. In *ICLR*, 2024. 7, 12
- [8] Xinlei Chen, Hao Fang, Tsung-Yi Lin, Ramakrishna Vedantam, Saurabh Gupta, Piotr Dollár, and C. Lawrence Zitnick. Microsoft COCO captions: Data collection and evaluation server. *CoRR*, abs/1504.00325, 2015. 3, 12, 14
- [9] Yen-Chun Chen, Linjie Li, Licheng Yu, Ahmed El Kholy, Faisal Ahmed, Zhe Gan, Yu Cheng, and Jingjing Liu. UNITER: universal image-text representation learning. In *ECCV*, pages 104–120, 2020. 14
- [10] Zuyao Chen, Jinlin Wu, Zhen Lei, Zhaoxiang Zhang, and Changwen Chen. Expanding scene graph boundaries: Fully open-vocabulary scene graph generation via visual-concept alignment and retention. In *ECCV*, 2024. 2, 5, 12, 14
- [11] Patrick Esser, Sumith Kulal, Andreas Blattmann, Rahim Entezari, Jonas Müller, Harry Saini, Yam Levi, Dominik Lorenz, Axel Sauer, Frederic Boesel, et al. Scaling rectified flow transformers for high-resolution image synthesis. In *ICML*, 2024. 1, 7, 12
- [12] Ying Fan, Olivia Watkins, Yuqing Du, Hao Liu, Moonkyung Ryu, Craig Boutilier, Pieter Abbeel, Mohammad Ghavamzadeh, Kangwook Lee, and Kimin Lee. Reinforcement learning for fine-tuning text-to-image diffusion models. *NeurIPS*, 2024. 1
- [13] Azade Farshad, Yousef Yeganeh, Yu Chi, Chengzhi Shen, Böjrn Ommer, and Nassir Navab. Scenegenie: Scene graph guided diffusion models for image synthesis. In *ICCV*, pages 88–98, 2023. 3, 7
- [14] Weixi Feng, Xuehai He, Tsu-Jui Fu, Varun Jampani, Arjun R. Akula, Pradyumna Narayana, Sugato Basu, Xin Eric Wang, and William Yang Wang. Training-free structured diffusion guidance for compositional text-to-image synthesis. In *ICLR*, 2023. 1, 2, 3, 7, 12
- [15] Weixi Feng, Wanrong Zhu, Tsu-jui Fu, Varun Jampani, Arjun Akula, Xuehai He, Sugato Basu, Xin Eric Wang, and William Yang Wang. Layoutgpt: Compositional visual planning and generation with large language models. *NeurIPS*, 2024. 3
- [16] Ian Goodfellow, Jean Pouget-Abadie, Mehdi Mirza, Bing Xu, David Warde-Farley, Sherjil Ozair, Aaron Courville, and Yoshua Bengio. Generative adversarial nets. In *NeurIPS*, pages 2672–2680, 2014. 1
- [17] Ian Goodfellow, Jean Pouget-Abadie, Mehdi Mirza, Bing Xu, David Warde-Farley, Sherjil Ozair, Aaron Courville, and Yoshua Bengio. Generative adversarial networks. *Communications of the ACM*, 63(11):139–144, 2020. 3
- [18] Jack Hessel, Ari Holtzman, Maxwell Forbes, Ronan Le Bras, and Yejin Choi. CLIPScore: A reference-free evaluation metric for image captioning. In *EMNLP*, pages 7514–7528, 2021. 1, 2, 6, 14
- [19] Martin Heusel, Hubert Ramsauer, Thomas Unterthiner, Bernhard Nessler, and Sepp Hochreiter. Gans trained by a two time-scale update rule converge to a local nash equilibrium. *NeurIPS*, 2017. 2, 6, 14
- [20] Jonathan Ho, Ajay Jain, and Pieter Abbeel. Denoising diffusion probabilistic models. *NeurIPS*, 33:6840–6851, 2020. 1
- [21] Phillip Isola, Jun-Yan Zhu, Tinghui Zhou, and Alexei A Efros. Image-to-image translation with conditional adversarial networks. In *CVPR*, pages 1125–1134, 2017. 1
- [22] Justin Johnson, Ranjay Krishna, Michael Stark, Li-Jia Li, David Shamma, Michael Bernstein, and Li Fei-Fei. Image retrieval using scene graphs. In *CVPR*, pages 3668–3678, 2015. 2
- [23] Justin Johnson, Agrim Gupta, and Li Fei-Fei. Image generation from scene graphs. In *CVPR*, pages 1219–1228, 2018. 3, 6, 14
- [24] Tero Karras, Samuli Laine, and Timo Aila. A style-based generator architecture for generative adversarial networks. In *CVPR*, pages 4401–4410, 2019. 1
- [25] Bahjat Kawar, Shiran Zada, Oran Lang, Omer Tov, Huiwen Chang, Tali Dekel, Inbar Mosseri, and Michal Irani. Imagic: Text-based real image editing with diffusion models. In *CVPR*, pages 6007–6017, 2023. 1

- [26] Diederik P. Kingma and Max Welling. Auto-encoding variational bayes. In *ICLR*, 2014. 1
- [27] Ranjay Krishna, Yuke Zhu, Oliver Groth, Justin Johnson, Kenji Hata, Joshua Kravitz, Stephanie Chen, Yannis Kalantidis, Li-Jia Li, David A Shamma, et al. Visual genome: Connecting language and vision using crowdsourced dense image annotations. *IJCV*, 123:32–73, 2017. 2, 3, 4, 5, 6
- [28] Alina Kuznetsova, Hassan Rom, Neil Alldrin, Jasper Uijlings, Ivan Krasin, Jordi Pont-Tuset, Shahab Kamali, Stefan Popov, Matteo Mallocci, Alexander Kolesnikov, et al. The open images dataset v4: Unified image classification, object detection, and visual relationship detection at scale. *IJCV*, 128(7):1956–1981, 2020. 3, 12
- [29] Kimin Lee, Hao Liu, Moonkyung Ryu, Olivia Watkins, Yuqing Du, Craig Boutilier, Pieter Abbeel, Mohammad Ghavamzadeh, and Shixiang Shane Gu. Aligning text-to-image models using human feedback. *CoRR*, abs/2302.12192, 2023. 1
- [30] Junnan Li, Dongxu Li, Silvio Savarese, and Steven Hoi. Blip-2: Bootstrapping language-image pre-training with frozen image encoders and large language models. In *ICML*, pages 19730–19742, 2023. 13
- [31] Haotian Liu, Chunyuan Li, Yuheng Li, Bo Li, Yuanhan Zhang, Sheng Shen, and Yong Jae Lee. Llava-next: Improved reasoning, ocr, and world knowledge, 2024. 14, 16
- [32] Haotian Liu, Chunyuan Li, Qingyang Wu, and Yong Jae Lee. Visual instruction tuning. *NeurIPS*, 2024. 6
- [33] Jinxiu Liu and Qi Liu. R3CD: Scene graph to image generation with relation-aware compositional contrastive control diffusion. In *AAAI*, pages 3657–3665, 2024. 3
- [34] Minghao Liu, Le Zhang, Yingjie Tian, Xiaochao Qu, Luoqi Liu, and Ting Liu. Draw like an artist: Complex scene generation with diffusion model via composition, painting, and retouching. *arXiv preprint arXiv:2408.13858*, 2024. 1, 3
- [35] Nan Liu, Shuang Li, Yilun Du, Antonio Torralba, and Joshua B Tenenbaum. Compositional visual generation with composable diffusion models. In *ECCV*, pages 423–439, 2022. 1, 3, 7, 12
- [36] Shilin Lu, Yanzhu Liu, and Adams Wai-Kin Kong. Tf-icon: Diffusion-based training-free cross-domain image composition. In *ICCV*, pages 2294–2305, 2023. 1
- [37] Jiayuan Mao. Scene graph parser. <https://github.com/vacancy/SceneGraphParser>, 2022. 2, 14
- [38] Alex Nichol, Prafulla Dhariwal, Aditya Ramesh, Pranav Shyam, Pamela Mishkin, Bob McGrew, Ilya Sutskever, and Mark Chen. Glide: Towards photorealistic image generation and editing with text-guided diffusion models. *arXiv preprint arXiv:2112.10741*, 2021. 1, 3
- [39] Dong Huk Park, Samaneh Azadi, Xihui Liu, Trevor Darrell, and Anna Rohrbach. Benchmark for compositional text-to-image synthesis. In *NeurIPS*, 2021. 3
- [40] Dustin Podell, Zion English, Kyle Lacey, Andreas Blattmann, Tim Dockhorn, Jonas Müller, Joe Penna, and Robin Rombach. SDXL: improving latent diffusion models for high-resolution image synthesis. In *ICLR*, 2024. 1, 6, 7, 12
- [41] Alec Radford, Jong Wook Kim, Chris Hallacy, Aditya Ramesh, Gabriel Goh, Sandhini Agarwal, Girish Sastry, Amanda Askell, Pamela Mishkin, Jack Clark, et al. Learning transferable visual models from natural language supervision. In *ICML*, pages 8748–8763, 2021. 14
- [42] Aditya Ramesh, Mikhail Pavlov, Gabriel Goh, Scott Gray, Chelsea Voss, Alec Radford, Mark Chen, and Ilya Sutskever. Zero-shot text-to-image generation. In *ICML*, pages 8821–8831, 2021. 3
- [43] Machel Reid, Nikolay Savinov, Denis Teplyashin, Dmitry Lepikhin, Timothy Lillicrap, Jean-baptiste Alayrac, Radu Soricut, Angeliki Lazaridou, Orhan Firat, Julian Schrittwieser, et al. Gemini 1.5: Unlocking multimodal understanding across millions of tokens of context. *arXiv preprint arXiv:2403.05530*, 2024. 3, 6, 12, 16
- [44] Robin Rombach, Andreas Blattmann, Dominik Lorenz, Patrick Esser, and Björn Ommer. High-resolution image synthesis with latent diffusion models. In *CVPR*, pages 10684–10695, 2022. 1, 3, 6, 7, 12
- [45] Tim Salimans, Ian Goodfellow, Wojciech Zaremba, Vicki Cheung, Alec Radford, and Xi Chen. Improved techniques for training gans. *NeurIPS*, 29, 2016. 6, 14
- [46] Shuai Shao, Zeming Li, Tianyuan Zhang, Chao Peng, Gang Yu, Xiangyu Zhang, Jing Li, and Jian Sun. Objects365: A large-scale, high-quality dataset for object detection. In *ICCV*, pages 8430–8439, 2019. 3, 12
- [47] Christian Szegedy, Vincent Vanhoucke, Sergey Ioffe, Jon Shlens, and Zbigniew Wojna. Rethinking the inception architecture for computer vision. In *CVPR*, pages 2818–2826, 2016. 14
- [48] Kaihua Tang, Hanwang Zhang, Baoyuan Wu, Wenhan Luo, and Wei Liu. Learning to compose dynamic tree structures for visual contexts. In *CVPR*, pages 6619–6628, 2019. 2
- [49] Ashish Vaswani, Noam Shazeer, Niki Parmar, Jakob Uszkoreit, Llion Jones, Aidan N. Gomez, Lukasz Kaiser, and Illia Polosukhin. Attention is all you need. In *NeurIPS*, pages 5998–6008, 2017. 6
- [50] Patrick von Platen, Suraj Patil, Anton Lozhkov, Pedro Cuenca, Nathan Lambert, Kashif Rasul, Mishig Davaadorj, Dhruv Nair, Sayak Paul, William Berman, Yiyi Xu, Steven Liu, and Thomas Wolf. Diffusers: State-of-the-art diffusion models. <https://github.com/huggingface/diffusers>, 2022. 12, 14
- [51] Peng Wang, Shuai Bai, Sinan Tan, Shijie Wang, Zhihao Fan, Jinze Bai, Keqin Chen, Xuejing Liu, Jialin Wang, Wenbin Ge, et al. Qwen2-vl: Enhancing vision-language model’s perception of the world at any resolution. *arXiv preprint arXiv:2409.12191*, 2024. 14, 16
- [52] Danfei Xu, Yuke Zhu, Christopher B. Choy, and Li Fei-Fei. Scene graph generation by iterative message passing. In *CVPR*, pages 3097–3106, 2017. 2
- [53] Tao Xu, Pengchuan Zhang, Qiuyuan Huang, Han Zhang, Zhe Gan, Xiaolei Huang, and Xiaodong He. Attngan: Fine-grained text to image generation with attentional generative adversarial networks. In *CVPR*, pages 1316–1324, 2018. 3
- [54] Ling Yang, Zhilin Huang, Yang Song, Shenda Hong, Guohao Li, Wentao Zhang, Bin Cui, Bernard Ghanem, and Ming-

- Hsuan Yang. Diffusion-based scene graph to image generation with masked contrastive pre-training. *arXiv preprint arXiv:2211.11138*, 2022. 7
- [55] Ling Yang, Zhaochen Yu, Chenlin Meng, Minkai Xu, Stefano Ermon, and CUI Bin. Mastering text-to-image diffusion: Recaptioning, planning, and generating with multi-modal llms. In *ICML*, 2024. 1, 3, 7, 12
- [56] Hu Ye, Jun Zhang, Sibio Liu, Xiao Han, and Wei Yang. IP-Adapter: Text compatible image prompt adapter for text-to-image diffusion models. *CoRR*, abs/2308.06721, 2023. 6
- [57] Keren Ye and Adriana Kovashka. Linguistic structures as weak supervision for visual scene graph generation. In *CVPR*, pages 8289–8299, 2021. 14
- [58] Rowan Zellers, Mark Yatskar, Sam Thomson, and Yejin Choi. Neural motifs: Scene graph parsing with global context. In *CVPR*, pages 5831–5840, 2018. 2, 14
- [59] Han Zhang, Tao Xu, Hongsheng Li, Shaoting Zhang, Xiaogang Wang, Xiaolei Huang, and Dimitris N Metaxas. Stackgan: Text to photo-realistic image synthesis with stacked generative adversarial networks. In *ICCV*, pages 5907–5915, 2017. 3
- [60] Yong Zhang, Yingwei Pan, Ting Yao, Rui Huang, Tao Mei, and Chang Wen Chen. Learning to generate language-supervised and open-vocabulary scene graph using pre-trained visual-semantic space. In *CVPR*, pages 2915–2924, 2023. 12, 14
- [61] Jun-Yan Zhu, Taesung Park, Phillip Isola, and Alexei A Efros. Unpaired image-to-image translation using cycle-consistent adversarial networks. In *ICCV*, pages 2223–2232, 2017. 1

---

**Algorithm 1** Generate Scene Graph

---

```
import google.generativeai as genai

generation_config = {
    "temperature": 0.7, "top_p": 0.95,
    "top_k": 64, "max_output_tokens": 8192,
    "response_mime_type": "application/json",
}

# Load the generative model
model = genai.GenerativeModel(
    "gemini-1.5-flash",
    generation_config=generation_config
)

prompt_template = """Given a set of detected
objects in an image, each object is
characterized by a name, a bounding box in "(
xmin, ymin, xmax, ymax)" format. Please
generate a scene graph to describe this image.
The scene graph should describe relationships
in the format "source -> relation -> target".
Example Output:\n{"relationships": [{"source":
"object_id1", "target": "object_id2", "relation
":\n"relation_type"}, ... ]}\n Now, objects are
{OBJECTS}. The original width and height of
the provided image are {IMG_WH}. Please output
the scene graph in JSON style without any
comments."""

def annotate(image_name):
    """
    image_name: file path of the image
    """
    # Load image and get its dimensions
    image = Image.open(image_name)
    image_wh = (image.width, image.height)

    # Load objects in the image,
    # e.g., [{"sports ball.1:[312, 360, 370,
    417]", "person.2:[116, 49, 309, 491]", "
    person.3:[367, 108, 550, 477]"}]
    image_objects = load_objects(image_name)

    # Construct text prompt
    text_prompt = prompt_template.replace(
        "OBJECTS", str(image_objects)).replace(
        "IMG_WH", str(image_wh))

    # Generate scene graph using generative model
    response = model.generate([
        image, text_prompt])
    return response
```

---

## A. MegaSG: a large-scale dataset of scene graphs

**Creation of the Dataset.** We create MegaSG by utilizing three object detection datasets: COCO [8], Object365 [46], and Open Images v6 [28]. The annotation prompt used to generate scene graphs from images is shown in Algorithm 1. **Scene Diversity.** To classify the scene categories, we utilize an LLM (e.g., Gemini 1.5 Flash [43]) to perform such

classification. The prompt used here is *Now, we have a list of image information like {IMAGE\_INFO}, where each image information contains “xyxy” bounding boxes and “relationships” depicting the relation between the “source” object and the “target” object. Please classify the scene in **each image** using the following hierarchy: Level 1: - People-Centric, - Non-People Centric. Level 2: If People-Centric: [Choose one: Social Interaction, Individual Activities, Work/Occupation, Travel/Exploration, Sports & Recreation, Performance/Entertainment, Daily Life]; If Non-People Centric: [Choose one: Nature, Urban/Built, Objects, Abstract/Artistic]. Please provide the classification for each image in the list, and present your answer as a **JSON-formatted** list of dictionaries, where each dictionary corresponds to an image and contains the following keys: “image\_id”, “file\_name”, “level 1”, “level 2”.*

Fig. 6 illustrates examples of categorized scenes in MegaSG, showcasing the diversity and range of scenarios covered in the dataset.

**Dataset Comparison.** To verify the quality of MegaSG, we trained two state-of-the-art SGG models, i.e., VS<sup>3</sup> [60] and OvSGTR [10]. Table 5 reports the zero-shot performance of these two models trained on MegaSG. From the result, MegaSG significantly improved the performance recall of OvSGTR from 22.79% to 45.71% (R@50, PredCls), offering a strong baseline to scale up SGG models. Beyond the SGG task, the vast and diverse scenes offer a valuable resource for training and evaluating diffusion models based on scene graphs.

We compare the word cloud of VG and MegaSG in Fig. 7. From the comparison in the word clouds, both the VG and MegaSG datasets contain similar high-frequency objects like “person”, “tree”, and “man”, as well as common relationships such as “on” and “near”. However, the MegaSG dataset shows a wider variety of object types and relationship terms, suggesting it captures a wider range of visual semantics than the VG dataset.

## B. Experiments

### B.1. Experimental Setup

**Models.** We evaluate several popular open-source diffusion models, including Composable [35], Structured [14], SD v1.5 [44] (checkpoint: *runwayml/stable-diffusion-v1-5*), SD v2.1 [44] (checkpoint: *stabilityai/stable-diffusion-2-1*), PixArt- $\alpha$  [7] (checkpoint: *PixArt-alpha/PixArt-XL-2-1024-MS*), SD3 [11] (checkpoint: *stabilityai/stable-diffusion-3-medium-diffusers*), SD3.5 [11] (checkpoint: *stabilityai/stable-diffusion-3.5-large*), SDXL [40] (checkpoint: *stabilityai/stable-diffusion-xl-base-1.0*), and LLM-based methods such as RPG [55]. We use *diffusers* [50] or official code to benchmark these models.

**Datasets.** We benchmark models on the widely used Visual

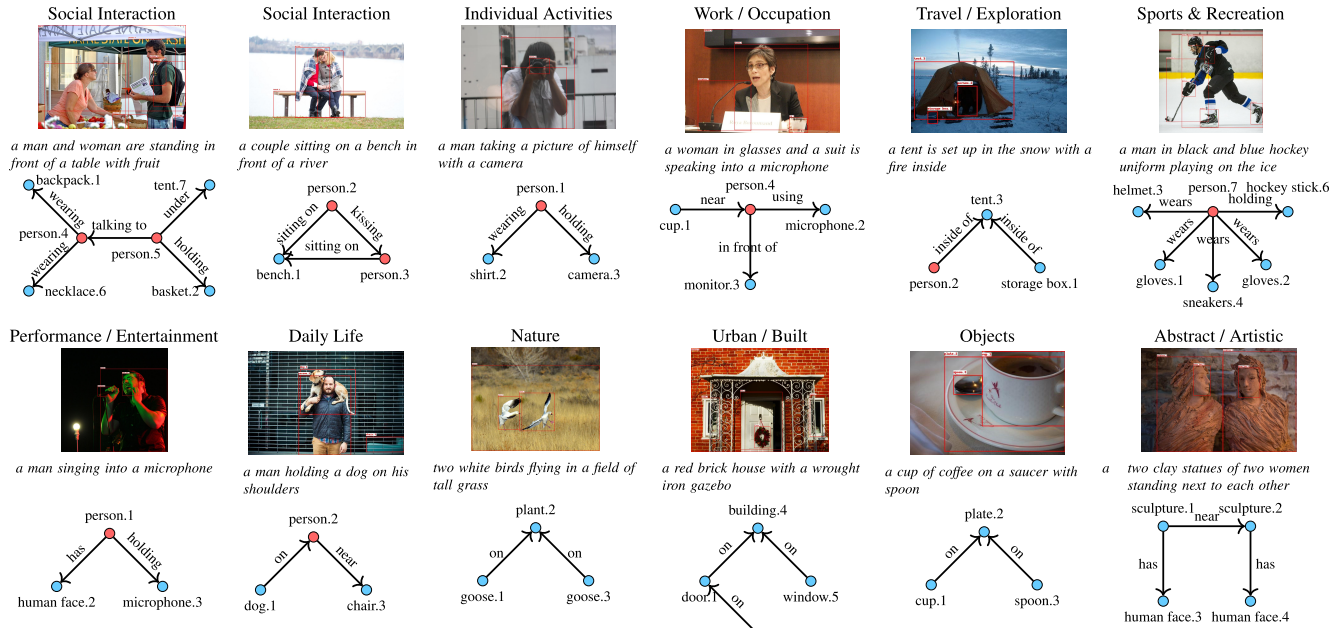


Figure 6. Illustration of scene categories in the MegaSG dataset. The image shows various themes, such as People-Centric (e.g., social interaction, individual activities) and Non-People-Centric (e.g., nature, urban environments). The caption is provided for illustrative purposes and generated using BLIP-2 [30], and the scene graph as described in Section 3.1.

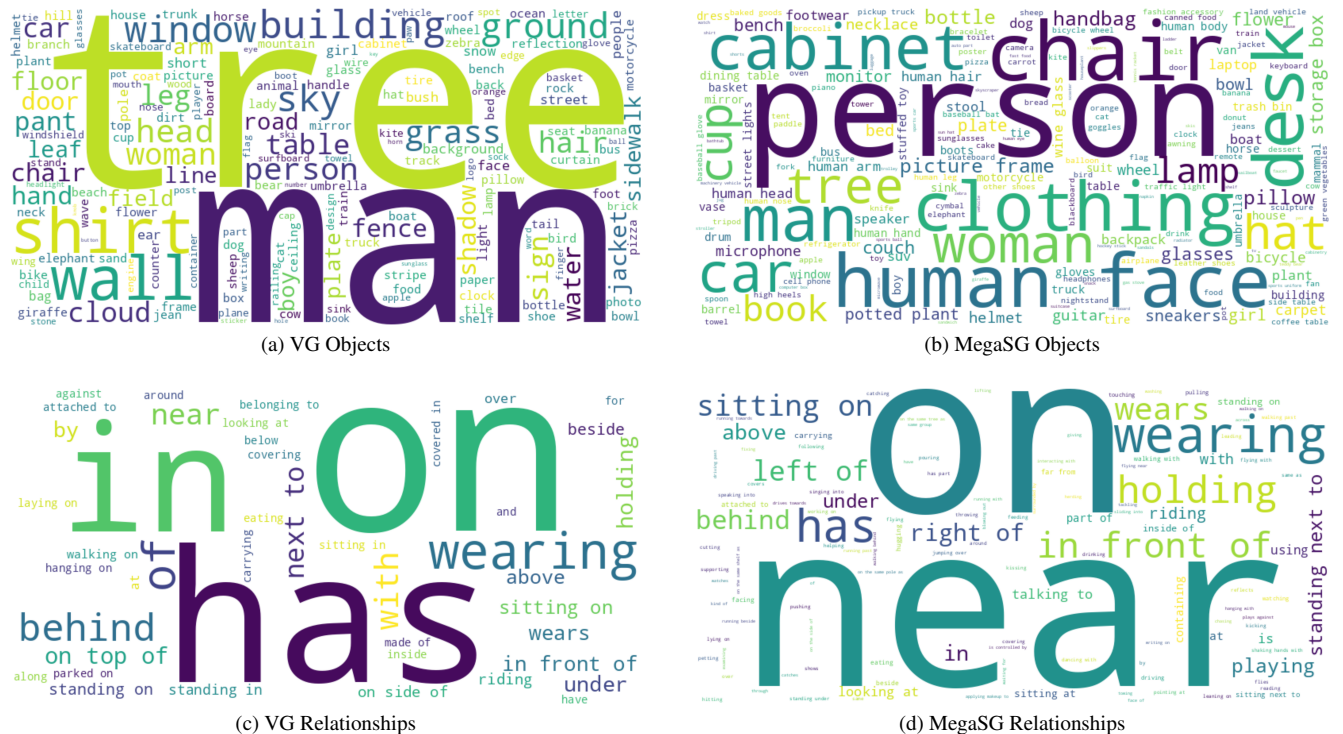


Figure 7. Word clouds of objects and relationships in the Visual Genome (VG) and MegaSG datasets. (a) and (b) illustrate the diversity of objects, while (c) and (d) highlight the relationships. The comparison demonstrates MegaSG’s broader vocabulary and richer representation of object-relationship semantics.

SGG model	Training Data	SGDet						PredCls					
		R@20/50/100			mR@20/50/100			R@20/50/100			mR@20/50/100		
LSWS [57]	COCO [8] Caption (104k)	-	3.28	3.69	-	-	-	-	-	-	-	-	-
MOTIFS [58]		5.02	6.40	7.33	-	-	-	-	-	-	-	-	-
Uniter [9]		5.42	6.74	7.62	-	-	-	-	-	-	-	-	-
VS <sub>(Swin-T)</sub> <sup>3</sup> [60]		4.56	5.79	6.79	2.18	2.59	3.00	12.30	16.77	19.40	3.56	4.79	5.51
VS <sub>(Swin-L)</sub> <sup>3</sup> [60]		4.82	6.20	7.48	2.29	2.70	3.09	12.54	17.28	19.89	3.57	4.83	5.56
OvSGTR <sub>(Swin-T)</sub> [10]		6.61	8.92	10.90	1.09	1.53	1.95	16.65	22.44	26.64	2.47	3.58	4.41
OvSGTR <sub>(Swin-B)</sub> [10]		6.85	9.33	11.47	1.28	1.79	2.18	16.82	22.79	27.04	2.94	4.24	5.26
VS <sub>(Swin-T)</sub> <sup>3</sup> [60]	MegaSG (644k)	5.56	8.19	10.17	1.15	1.71	2.20	23.81	29.64	32.18	4.70	5.96	6.57
VS <sub>(Swin-L)</sub> <sup>3</sup> [60]		9.74	14.80	18.80	1.57	2.71	3.75	31.88	38.77	41.76	5.32	6.88	7.58
OvSGTR <sub>(Swin-T)</sub> [10]		<b>9.94</b>	<b>13.92</b>	<b>17.17</b>	<b>3.05</b>	<b>4.03</b>	<b>4.76</b>	<b>37.12</b>	<b>44.10</b>	<b>47.09</b>	<b>8.49</b>	<b>10.22</b>	<b>11.07</b>
OvSGTR <sub>(Swin-B)</sub> [10]		<b>10.63</b>	<b>14.93</b>	<b>18.36</b>	<b>3.01</b>	<b>4.10</b>	<b>4.99</b>	<b>38.72</b>	<b>45.71</b>	<b>48.51</b>	<b>8.38</b>	<b>10.31</b>	<b>11.07</b>

Table 5. Zero-shot performance of state-of-the-art methods on the VG150 test set. For the COCO Caption dataset, a language parser [37] has been used for extracting triplets from the caption. To prevent information leakage, we sampled 644k images from MegaSG, ensuring that the CLIP similarity of each sampled image with the VG test set remained below 0.9.

Genome (VG) and the proposed MegaSG dataset.

- VG consists of 108k images annotated by human. Following SG2Im [23], it has been split into training set (62,565), validation set (5,506), and test set (5,088<sup>1</sup>) images for scene graph-based image generation.
- MegaSG comprises 1 million images annotated using Gemini 1.5 Flash. Relationships with a frequency below 100 are filtered out, and synonyms are merged by a large language model (LLM).

**Metrics.** We employ common metrics and the proposed SGScore.

- Inception Score (IS) [45]: Measures the realism of generated images using a pre-trained Inception-V3 [47] network.
- Fréchet Inception Distance (FID) [19]: Assesses the similarity between generated and real images by measuring the distance between the distributions of their feature representations.
- CLIPScore [18]: Evaluates the semantic alignment between generated images and corresponding text using the CLIP model [41].
- SGScore measure the factual consistency in terms of object recall and relation recall. We use  $\alpha = 0.5$  in Eq. (4) of Section 3.2 to give a balanced measurement.

**Scene Graph Representation and Complexity.** We define the scene complexity of a scene graph  $G = (V, E)$  as:

$$C(G) = \gamma \cdot |V| + (1 - \gamma) \cdot |E|, \quad (6)$$

where  $\gamma$  is a weighting factor. The three levels of complexity are defined as follows:

- **Simple:**  $1 \leq C(G) \leq 3$ , typically involving 2–3 objects and no more than 3 relationships in the scene.
- **Medium:**  $4 \leq C(G) \leq 7$ , characterized by a denser arrangement of objects and relationships.

<sup>1</sup>we use official code to obtain 5,096 images for test.

- **Hard:**  $C(G) \geq 8$ , representing the most challenging cases with highly dense objects and intricate relationships.

**LLM.** In addition to utilizing Gemini 1.5 Flash, we also present results using GPT-4o [1], Qwen-VL-Max [51], and LLaVA 1.5 [31] to evaluate the robustness of the proposed SGScore.

**IP-Adapter.** We use the official implementation in `diffusers` [50], with  $\lambda_0$  and  $\lambda_1$  (in Eq. (5) of Sec. 4) empirically set to 0.5.

## B.2. Evaluation of Scene-Bench

**Impact of Scene Complexity.** To examine how scene complexity affects model performance, we analyzed FID and SGScore for SD v1.5, SD v2.1, SDXL, and our model across various complexity levels (see Fig. 8).

As scene complexity increases (*i.e.*, with more objects and relationships), we observe a consistent decline in SGScore across all models. This suggests that, with greater complexity, the models struggle to accurately represent the expected scene graphs. The decreasing SGScore highlights the challenge of maintaining factual consistency in complex scenes. However, our model demonstrates a notable improvement over the other models by consistently achieving a higher SGScore across all complexity levels, particularly through maintaining stable and high object recall. This suggests that our model is more effective at preserving factual consistency even in complex scenes.

Interestingly, FID scores remain stable across complexity levels, indicating that image quality does not degrade significantly with complexity. This stability implies that while models retain visual fidelity, they encounter difficulties modeling intricate object relationships and interactions in complex scenes. Therefore, even as images appear visually coherent, the factual accuracy, as measured

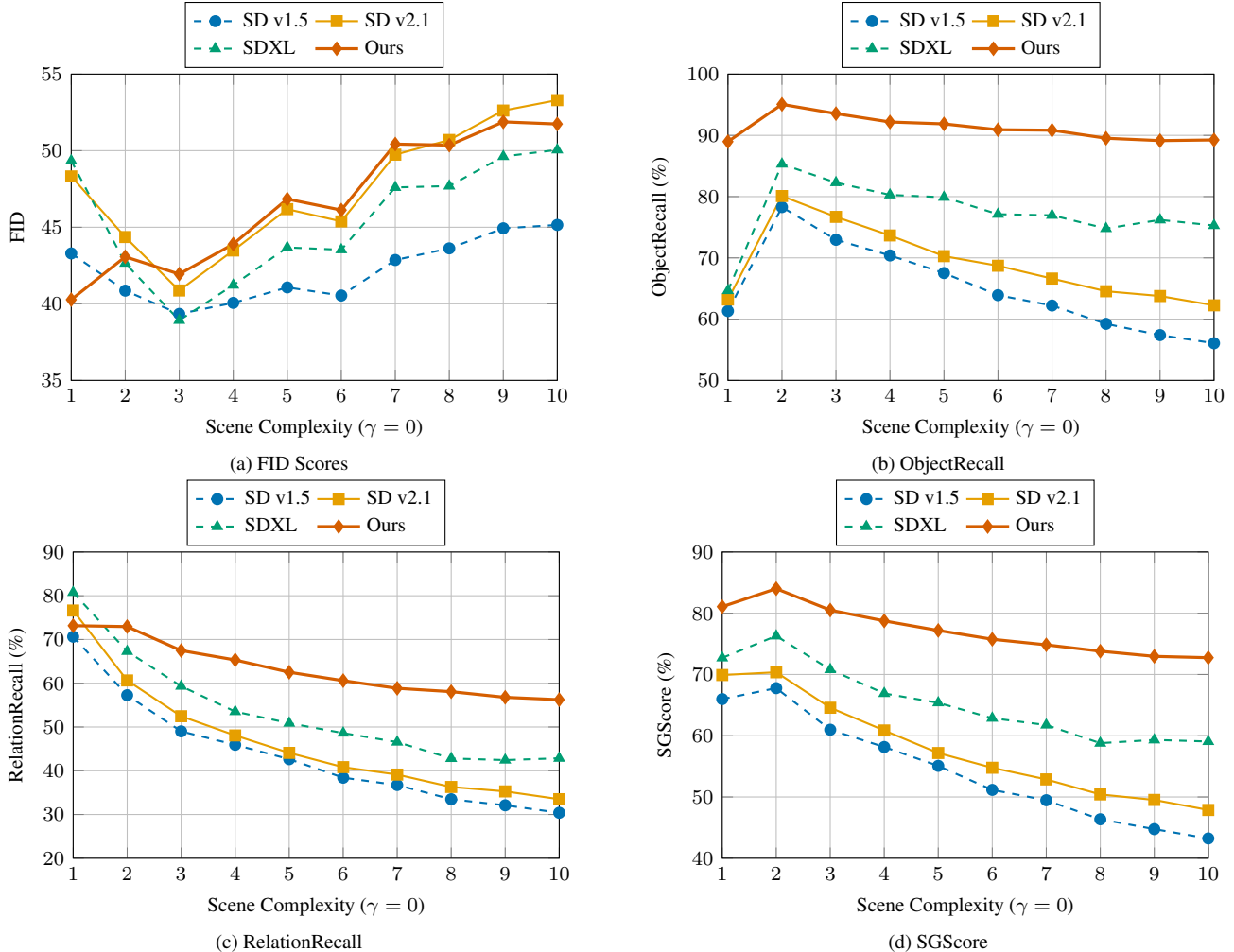


Figure 8. Comparison of FID, ObjectRecall, RelationRecall, and SGScore for models SD v1.5, SD v2.1, SDXL, and Ours across different scene complexity levels. (a) FID scores show relatively stable image quality, while (b) ObjectRecall and (c) RelationRecall indicate a consistent decline in factual consistency with increasing scene complexity. (d) SGScore demonstrates the overall advantage of our approach in maintaining higher factual consistency, particularly in complex scenes.

by SGScore, declines with increased scene complexity.

### B.3. Evaluation of Scene Graph Feedback

**Additional Ablation Study.** To evaluate the effectiveness of the scene graph feedback, particularly considering the additional parameters introduced by the IP-Adapter, we conducted another ablation study. In this experiment, we set  $\lambda_1 = 0$  in Eq. (5) of Sec. 4, meaning the IP-Adapter processes only the initial generated image, without incorporating the reference image derived from the missing graph.

As shown in Tab. 6, introducing the IP-Adapter alone (row 2 vs. row 1) does not improve the factual consistency of generated images. However, incorporating the reference image (row 3) significantly enhances ObjectRecall, RelationRecall, and SGScore, demonstrating the importance of

IP-Adapter	Reference Image	ObjectRecall	RelationRecall	SGScore
✗	✗	75.45	48.84	62.14
✓	✗	70.91	49.83	60.37
✓	✓	<b>79.93</b>	<b>53.97</b>	<b>66.95</b>

Table 6. Comparison of ObjectRecall, RelationRecall, and SGScore with and without the reference image in the IP-Adapter setup.

scene graph feedback.

### B.4. Human Evaluation

We conducted a human evaluation to assess the effectiveness of SGScore in verifying factual consistency. Specifically, three human annotators were instructed to select the

Select the candidate image that best matches the original image based on object alignment and relationships

Original Image



Candidates

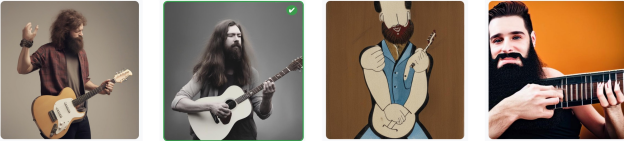


Select the candidate image that best matches the original image based on object alignment and relationships

Original Image



Candidates

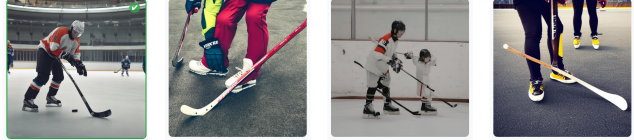


Select the candidate image that best matches the original image based on object alignment and relationships

Original Image



Candidates



Select the candidate image that best matches the original image based on object alignment and relationships

Original Image



Candidates

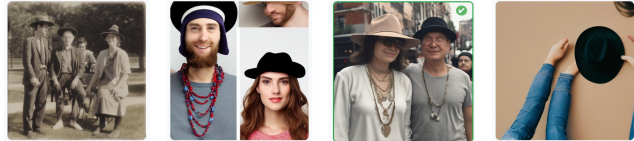


Figure 9. Example questions presented to human annotators.

candidate image that best aligns with the original image regarding object presence and relationship accuracy. We randomly sampled 1,000 images and selected corresponding generated images from four models: SD v1.5, SD v2.1, SDXL, and Ours (SDXL). Model identities were hidden from the annotators to avoid bias. Fig. 9 illustrates the annotation interface.

## C. Additional Results

### C.1. Multimodal LLMs for SGGScore

We evaluate the performance of different multimodal LLMs on SGGScore, including Gemini 1.5 Flash [43], GPT-4o [1], Qwen-VL-Max [51], and LLaVA 1.5 [31], as shown in Fig. 10. The results show minimal discrepancies across models, indicating that SGGScore is insensitive to the specific choice of state-of-the-art multimodal LLMs for the same evaluation. However, the visual reasoning capability of these models remains important. Considering cost-effectiveness, we recommend Gemini 1.5 Flash, which of-

fers excellent multimodal reasoning performance at a significantly lower price [2].

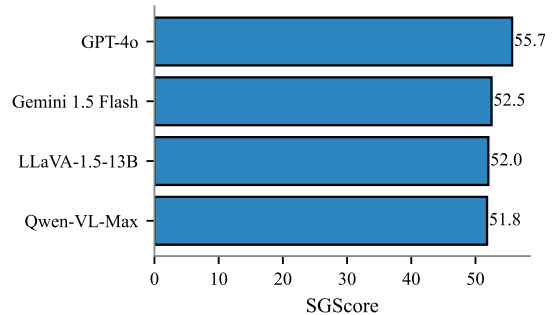


Figure 10. Performance comparison of M-LLMs on VG test set (images are generated by SD v1.5).



## C.2. Sensitivity Analysis of SGGScore

To test the scalability and sensitivity of SGGScore, we randomly sample subsets (*e.g.*, with size 500, 1k, 2k, 4k,  $\dots$ , 32k, *etc.*) from the MegaSG to compute the SGGScore on images generated by SD v1.5. As shown in Fig. 11, the mean SGGScore remains relatively stable across sample sizes, with only slight variations observed. Additionally, the standard deviation decreases as the sample size increases, demonstrating that the metric becomes more reliable and less sensitive to random fluctuations with larger subsets. This indicates that SGGScore is both scalable and robust, providing consistent evaluations of factual consistency regardless of the dataset size.

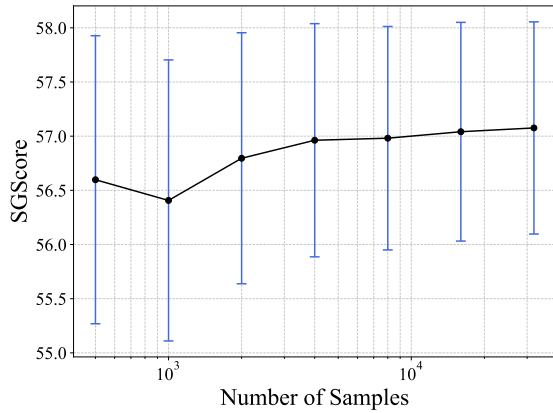


Figure 11. Mean and standard deviation (std.) of SGGScore across varying numbers of samples. For each sample size, the image generation process is repeated with different random seeds using SD v1.5 to compute the mean and std. of SGGScore.